# Chemically Enhanced Convective Dissolution of CO2

R. Tanaka, C. Almarcha, Y. Nagatsu, Yves Méheust, Patrice Meunier

# Chemically enhanced convective dissolution of $CO_2$

R. Tanaka,[1] C. Almarcha,[2] Y. Nagatsu,[1] Y. Méheust,[3] and P. Meunier[2,*]

[1] *Department of Chemical Engineering, Tokyo University of Agriculture and Technology, 2-24-16 Naka-cho, Koganei, Tokyo 184-8588, Japan*

[2] *Aix Marseille Université, CNRS, Centrale Marseille, IRPHE UMR 7342, 13384 Marseille, France*

[3] *Univ Rennes, CNRS, Géosciences Rennes, UMR 6118, 35000 Rennes, France*

(Dated: January 12, 2024)

Convective dissolution, one of the main mechanisms for geological storage of $CO_2$, occurs when supercritical or gas $CO_2$ dissolves partially into an aqueous solution, thus triggering downward convection of the denser $CO_2$-enriched liquid. Chemical reaction in the liquid can greatly enhance the process. Here, experimental measurements of convective flow inside a cylinder filled with a sodium hydroxide (NaOH) solution show that the plume's velocity can be increased tenfold as compared to a situation with no NaOH. This tremendous effect is predicted by a model with no adjusting parameters.

The interplay between chemical reactions and hydrodynamic convection can lead to a rich variety of phenomena. These are triggered by the control of chemical reactions on parameters that directly impact the local mobility of the fluid during natural convection [1], namely the fluid's density [2] or viscosity [3], the molecular diffusivities of the reactants and products [4, 5], or, in porous media flow and for chemical reactions involving the solid phase, the medium's permeability [6]. Such effects can allow chemical reactions to accelerate convection [7, 8] and even, in otherwise hydrodynamically-stable configurations, to trigger hydrodynamic instabilities [9]. Conversely, the convection leads to enhancement of the diffusion process due to enhanced fluid stretching, which generally increases concentration gradients transverse to the stretching direction, thus resulting in larger reaction rates for diffusion-limited reactive configurations [10–12].

Natural convection of dissolved carbon dioxide ($CO_2$) within the aqueous phase of deep subsurface permeable media (aquifers and depleted hydrocarbon reservoirs) is at the core of one of the four main mechanisms of $CO_2$ subsurface trapping, namely dissolution trapping [13]. It allows $CO_2$ captured from industrial operations to be stored in the subsurface by gravity over a time scale far extending the mean atmospheric residence time of $CO_2$, and is thus considered as a major potential mitigation measures towards decreasing atmospheric $CO_2$ concentration and limiting the associated raise in atmospheric temperatures. In this context, the injected $CO_2$ is in its supercritical phase, and thus rises by buoyancy to position itself above the resident aqueous phase (a brine); it then dissolves partially into it [14] through the $sCO_2$-brine interface. The mixture layer thus created at the top of the aqueous phase is denser than the brine underneath, which leads to a Rayleigh-Taylor instability [9, 15]. The resulting convection fuels the continuous dissolution of $sCO_2$ into $CO_2$-devoid brine coming up from the bottom of the geological formation. This so-called convective dissolution has been investigated extensively both experimentally and numerically in the past 15 years in the absence of chemical reactions [13, 16–21], but investigations of the net effect of chemical reactions that can take place in the aqueous phase remain to be complemented. The influence of acid-base reactions on convection during dissolution of $CO_2$ has been analyzed in several studies [7, 22, 23], focusing on the roles of different densities and molecular diffusivities of the product and reactants in A + B $\longrightarrow$ C reactions. Thomas *et al.* [24] showed that adding a base XOH to the aqueous phase accelerated convective dissolution in a Hele-Shaw cell, and compared this effect for different spectators ions X. These studies [7, 22–24] were mostly limited to the early stages of destabilization, from the onset of convection in the linear regime to the early stages of fingering.

Here, we address the impact of the aqueous phase's basicity on the convective dissolution of $CO_2$ in the aqueous phase. Many previous studies have investigated the impact of chemical reactions on convection in a liquid phase when the reaction takes place at the interface between the liquid and another phase (usually, a gas) [25–27], but the effect of the solution's basicity on the dissolution's chemical equilibrium itself, and the resulting impact on natural convection within the liquid, has to our knowledge only been addressed in a Hele-Shaw configuration and during initial fingering stages [24]. Here, using a dedicated experiment and sodium hydroxide (NaOH) to render the aqueous phase basic, we demonstrate that the resulting enhancement of convection in the fully nonlinear late-time convection regime can reach a factor 20. This convection enhancement is measured in terms of the maximum dissolved $CO_2$ plume velocity as a function of the NaOH concentration and of the pressure of gaz $CO_2$, and compared to a theoretical prediction, with very good agreement. These results are to our knowledge the first insights into the acceleration of convective dissolution dynamics in the constant flux regime, which is expected to have the strongest impact on the global dynamics of $CO_2$ dissolution storage in the subsurface.

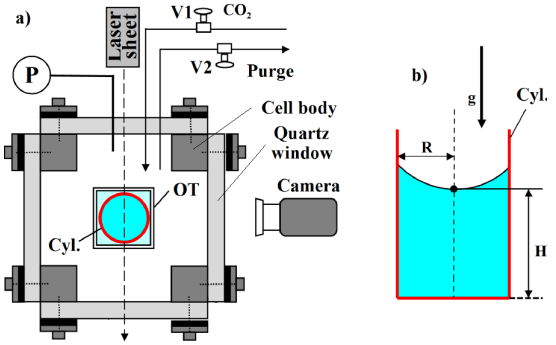


FIG. 1. (a) Top view of the experimental setup where the cylindrical flow cell (Cyl., red online) is immersed in the cuboid optical tank and located in the cubic pressure cell. (b) Close-up side view of the cylindrical cell with the solution exhibiting a meniscus.

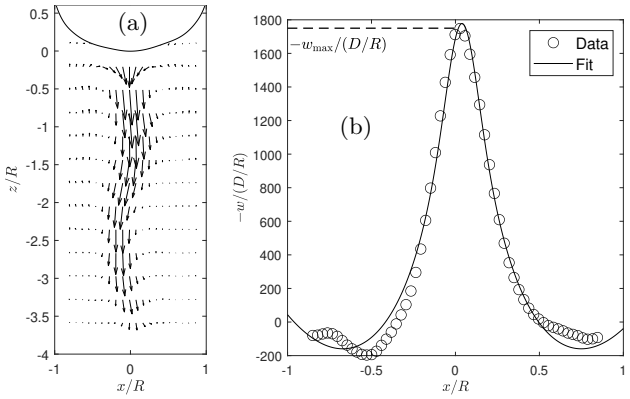


FIG. 2. (a) Velocity field obtained for $P_{CO_2} = 0.3$ bar and $C_{NaOH} = 0.1$ M at time $t = 120$ s.). (b) Radial profile of the vertical velocity component $w$ at depth $z = -R$, obtained for $P_{CO_2} = 0.3$ bar and $C_{NaOH} = 0.1$ M at $t = 120$ s. The solid line corresponds to the viscous solution given in Eq.(1). The vertical component of the velocity is negative for sufficiently large radial positions, and the flow rate calculated over the entire cross section is zero, as required by fluid mass conservation. $D$ is the molecular diffusivity of $CO_2$ in water. The Rayleigh number defined by (4) is $Ra_0 = 4.3 \times 10^4$.

To obtain a quasi-stationary flow in the non-linear convection regime, the experiments are performed on a single plume of dissolved $CO_2$, in a cylindrical glass container of radius $R = 4$ mm (see Fig. 1) filled with water and sodium hydroxide (NaOH) up to a height $H = 16$ mm (see detailed description of the setup in Nadal et al. [28]). The tube is immersed in a square optical tank containing the same solution (to reduce radial distortions of the images) and placed at the center of a pressure cell which is filled in a few seconds with gaseous $CO_2$ at a partial pressure $P_{CO_2}$, chosen equal to 0.1, 0.3 and 1 bar in three distinct series of experiments. In each series the concentration $C_{NaOH}$ in sodium hydroxide is varied from 0 to 5M (mol/l). Upon $CO_2$ injection (which defines the initial time $t = 0$), the denser layer of $CO_2$-enriched solution destabilizes as explained above and sinks towards the bottom of the cylinder, generating a strong plume close to the axis of the cylinder, surrounded by a weak upward recirculating flow. Particle image velocimetry (PIV) [29] measurements are performed to measure the velocity field, by seeding the fluid with 6 µm diameter spheres of red-dyed polystyrene and illuminating the flow cell along a diametral plane by a 150 µm thick red laser sheet. A typical velocity field obtained during the convection is shown in Fig. 2(a).

An example of profile of the vertical velocity component $w$ as a function of the distance $r$ to the axis of the cylindrical cell is plotted in Fig. 2(b). It is favorably compared to the theoretical profile $w(r)$ of a single viscous plume in the container[28], characterized by its maximum velocity $w_{max}$ and its thickness $l$:

$$w(r) = -w_{max} \frac{F_l(r/R)}{F_l(0)} \qquad (1)$$

$$\text{with} \quad F_l(y) = \int_{y/l}^{1/l} \frac{1 - e^{-x^2}}{x} dx + (y^2 - 1)(1 - l^2).$$

Note that this radial distribution of the velocity's vertical component verifies the conservation of the fluid mass, which is one of the first principles taken into account when deriving Eq. (1). Hence, $\int_0^R w(r)\, r dr = 0$. This is actually rigorously true in the limit of small $l$ values (here $l \simeq 0.1$). see Ref. [28] for more details.

Fitting Eq. (1) to the data (solid line in Fig. 2b), the maximum vertical velocity $w_{max}$ is extracted and plotted as a function of time for two different NaOH concentrations (Fig. 3). In the absence of NaOH (dashed line), after a transient stage (i.e. after $t \approx 0.05R^2/D$ here, where $D$ is the molecular diffusivity of $CO_2$ in water) $w_{max}$ becomes almost stationary. In the presence of sodium hydroxide (solid line), $w_{max}$ increases strongly over a very short time and then decreases slowly with time (by about 50% during the experiment). The striking fact that at 0.1 M (solid line) $w_{max}$ remains 4 times larger than in the absence of sodium hydroxide for half the experimental time evidences the strong influence of pH and chemical reactions on the convection induced by $CO_2$ dissolution. In the presence of NaOH $w_{max}$ oscillates around its mean valuedue to instabilities occurring for larger Rayleigh numbers [30] and that may be enhanced by the presence of NaOH. Note that the non-dimensional velocity $w_{max}R/D$ can be viewed as a global Péclet number based on the plume's velocity and the global length scale $R$.

The maximum vertical velocity component is extracted at the beginning of the quasi-stationary stage (i.e. for $tD/R^2$ larger than 0.05) for several concentrations $C_{NaOH}$ and three different $P_{CO_2}$ (see Fig. 4). At low concentrations ($C_{NaOH} \lesssim 3 \times 10^{-4}$ M), the plume's velocity

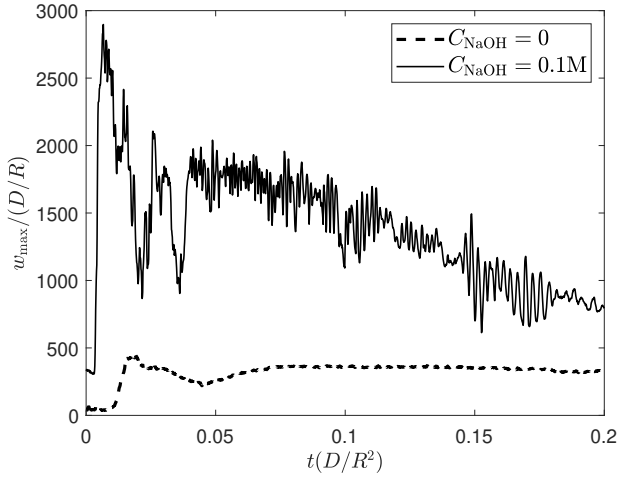


FIG. 3. Maximum velocity obtained for $P_{\mathrm{CO}_2} = 0.3$ bar with $C_{\mathrm{NaOH}} = 0$ (dashed line) and $C_{\mathrm{NaOH}} = 0.1$ M (solid line). The Rayleigh number defined by (4) is $Ra_0 = 4.3 \times 10^4$.

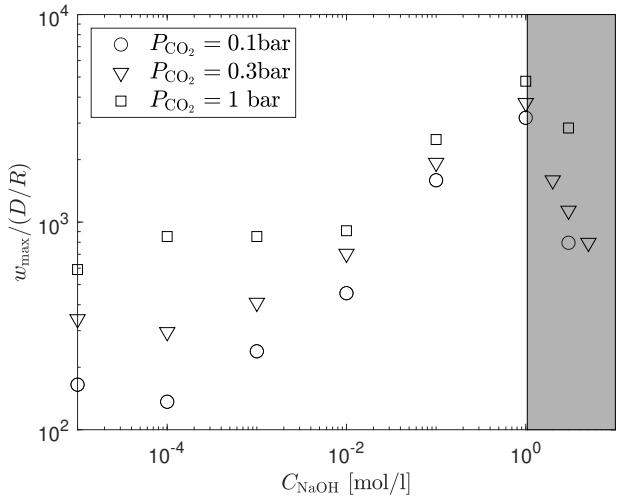


FIG. 4. Maximum vertical velocity component as a function of $C_{\mathrm{NaOH}}$, obtained for $P_{\mathrm{CO}_2} = 0.1\,\mathrm{bar}$ (◯, $Ra_0 = 1.4 \times 10^4$), $P_{\mathrm{CO}_2} = 0.3\,\mathrm{bar}$ (▽, $Ra_0 = 4.3 \times 10^4$) and $P_{\mathrm{CO}_2} = 1\,\mathrm{bar}$ (□, $Ra_0 = 1.4 \times 10^5$).

dependence on $P_{\mathrm{CO}_2}$ is the one already obtained experimentally in the absence of sodium hydroxide [28]. From $C_{\mathrm{NaOH}} = 10^{-3}$ M, $w_{\max}$ increases significantly with the sodium hydroxide concentration, up to a factor ten when $C_{\mathrm{NaOH}} = 1$ M. Above $C_{\mathrm{NaOH}} = 1$ M, $w_{\max}$ saturates and decreases rapidly (zone coloured in grey).

In the following, we present a model predicting this dependence of the plume's velocity on $P_{\mathrm{CO}_2}$ and $C_{\mathrm{NaOH}}$.

In pure water, dissolved $CO_2$ is barely unstable [31] and we can neglect the reactions $CO_2 + H_2O \rightleftharpoons H_2CO_3$ and $H_2C0_3 \rightleftharpoons H^+ + HCO_3^-$ (the first one being the limiting reaction). In such non reactive conditions, the spatial distribution of the $CO_2$ concentrations is well described by a vertical diffusion profile $C(r,z) = 1 - \mathrm{erf}(z/\delta(r))$ [28]. The dependence on the radial coordinate $r$ of the diffusive width $\delta$, which is due to advection by the (radial) velocity at the gas-liquid interface, was predicted analytically by Nadal et al. [28]. However, in a basic solution, the successive reactions $CO_2 + OH^- \rightleftharpoons HCO_3^-$ and $HCO_3^- + OH^- \rightleftharpoons CO_3^{2-} + H_2O$ take place, the first one being the limiting irreversible reaction, and the second one being much faster and reversible. Depending on the local pH, either the $CO_2$ (for pH<6.4), $HCO_3^-$ (for 6.4<pH<10.3), or $CO_3^{2-}$ (for pH>10.3) forms will be predominant.

For moderate initial concentrations in NaOH (less than $10^{-3.7}$) we can expect the presence of $HCO_3^-$ in the bulk. Still, the $CO_2$ form should be present close to the surface, where the fluid is depleted in NaOH. For high concentrations in NaOH (more than $10^{-3.7}$) we can expect the presence of $CO_3^{2-}$ in the bulk, $HCO_3^-$ closer to the surface, where reaction induces a depletion in $OH^-$, and still some $CO_2$ in the vicinity of the surface [32]. In fact, the theoretical configuration in the absence of convection features two horizontal planes at which the concentrations of the two species involved in the equilibria ($CO_2$ and $HCO_3^-$ for the first plane, $HCO_3^-$ and $CO_3^{2-}$ for the second one) are identical [33] (see also Fig. S1 in the Supp. Mat.). In the presence of convection, these isoconcentration positions are decreasing functions of the radial coordinate $r$, due (again) to advection by the radial velocity at the free surface. The integration of that model gives us the density excess in the fluid, which will be used in the following to derive the plume's velocity.

For very high concentration in $HCO_3^-$, precipitation of sodium bicarbonate $NaHCO_3$ at the liquid-gas interface creates a thin crust which is observed in our experiment. This probably inhibits the dissolution of $CO_2$, leading to a drastic reduction of the plume's velocity for $C_{\mathrm{NaOH}} >$ 1.04 M (as given by a solubility of 87g/l for $HCO_3^-$). This region (coloured in grey in Fig. 4) is not considered in the following.

In the absence of sodium hydroxide, Nadal et al. [28] showed theoretically that the plume's velocity is :

$$w_0^{\mathrm{th}} = 0.115\ Ra_0^{2/3}\ \left[\log(Ra_0)\right]^{1/3} \frac{D}{R}, \tag{2}$$

and the plume's width is

$$l_0^{\mathrm{th}} = 1.359\ Ra_0^{-1/6}\ \left[\log(Ra_0)\right]^{-1/3} R, \tag{3}$$

where the Rayleigh number $Ra_0$ is defined as

$$Ra_0 = \frac{\alpha k_{\mathrm{H}} P_{\mathrm{CO}_2} g R^3}{D\nu}. \tag{4}$$

Here $g = 9.81\mathrm{m}^2\,\mathrm{s}^{-2}$ is the gravity, $D = 1.8\times10^{-9}\mathrm{m}^2\,\mathrm{s}^{-1}$ is the molecular diffusivity of $CO_2$ in water, and $\nu$ is the kinematic viscosity of the liquid (taking into account the increase due to the presence of NaOH). $k_{\mathrm{H}} = 3.4 \times 10^{-2}$

M/atm is the Henry's constant for $CO_2$ dissolution in water, and $\alpha = (1/\rho)(\partial\rho/\partial C) = 0.011\mathrm{M}^{-1}$ is the chemical expansion coefficient, $C$ being the concentration in dissolved $CO_2$ [see 34]. In this definition the term $\alpha k_H P_{CO_2}$ corresponds to the liquid's density increase at the liquid-gas interface due to absorption of $CO_2$ through the interface. Note that, in addition to the aforementioned global Péclet number $wR/D$, it is also interesting to define a local Péclet number quantifying the ratio of the radial diffusive time scale over the plume's width $l$ to the advective time scale $l/w$ :

$$Pe_0 = \frac{w_0^{\mathrm{th}}\, l_0^{\mathrm{th}}}{D} = 1.156\,\sqrt{Ra_0}\ . \tag{5}$$

In the presence of sodium hydroxide, the variations in density are now due to the presence of the reactants $CO_2$, $HCO_3^-$ and $CO_3^{2-}$, but also to local variations in the concentrations of the ions $OH^-$ (which have reacted) and $Na^+$. Thomas et al. [24] investigated the high concentration in the NaOH case, and assumed that the concentration of $OH^-$ was large so that the $HCO_3^-$ form was not present. They thus assumed that the density difference was mostly due to the presence of $CO_3^{2-}$, characterized by a chemical expansion coefficient $\alpha'$. Since the concentration of $CO_3^{2-}$ is limited by the sodium hydroxide concentration, the density difference in the plume reduces to $\alpha k_H P_{CO_2} + \alpha' C_{NaOH}$. As a consequence, in the presence of sodium hydroxide, the Rayleigh number should be defined as

$$\begin{aligned} Ra &= \frac{(\alpha k_H P_{CO_2} + \alpha' C_{NaOH}) g R^3}{D\nu} \\ \text{i.e.,}\quad Ra &= Ra_0 \left(1 + \frac{\alpha' C_{NaOH}}{\alpha k_H P_{CO_2}}\right). \end{aligned} \tag{6}$$

The theoretical velocity of the plume is then given by Eq. (2) with $Ra_0$ replaced by the Rayleigh number $Ra$ defined above.

The ratio of the velocity in the presence of NaOH to that in the absence of NaOH is thus equal to

$$\frac{w^{\mathrm{th}}}{w_0^{\mathrm{th}}} = \Gamma\left(1 + \frac{\alpha' C_{NaOH}}{\alpha k_H P_{CO_2}}\right)^{2/3} \tag{7}$$

where the coefficient $\Gamma$ takes into account the logarithmic dependencies : it varies between 1 and 1.17 for the experiments considered in this study. This law is plotted in Fig. 5 for $\Gamma = 1$ and $\alpha'/\alpha = 0.85/0.82$ as predicted by [24] when taking into account only the solutal effects (known from the tables of the literature). This prediction is in good agreement with the experimental results, which all collapse when plotting $w^{\mathrm{th}}/w^{\mathrm{th}_0}$ as a function of $C_{NaOH}/(k_H P_{CO_2})$. However, the theory slightly underestimates the velocity at moderate concentrations probably due to diffusive effects which can increase the value of $\alpha'/\alpha$, as described by [24]. Their figure 13 indicates

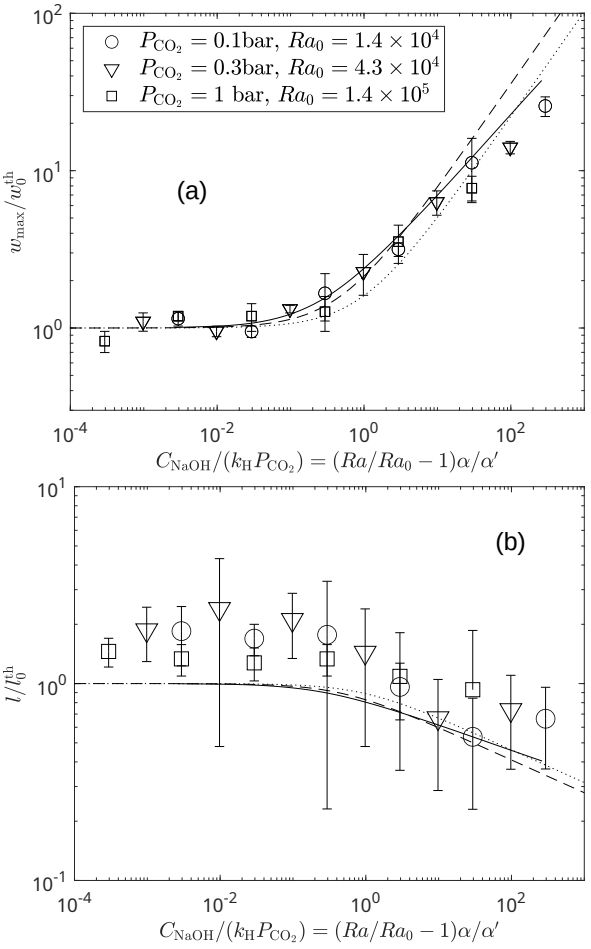


FIG. 5. (a) Maximum vertical velocity component, normalized by the theoretical velocity $w_0^{\mathrm{th}}$ at $C_{NaOH} = 0$ given by Eq. (2). (b) Plume width, normalized by the theoretical plume width $l_0^{\mathrm{th}}$ at $C_{NaOH} = 0$ given by Eq. (3). Symbols correspond to $P_{CO_2} = 0.1\,\mathrm{bar}$ (◯, $Ra_0 = 1.4 \times 10^4$), $P_{CO_2} = 0.3\,\mathrm{bar}$ (▽, $Ra_0 = 4.3 \times 10^4$) and $P_{CO_2} = 1\,\mathrm{bar}$ (□, $Ra_0 = 1.4 \times 10^5$). The dotted lines correspond to the theoretical ratio given by Eq. (7) and (8) with $\alpha'/\alpha = 0.85/0.82$. The dashed lines are for $\alpha'/\alpha = 2.12$. The solid lines use values of $\alpha'/\alpha$ calculated for each concentration and pressure from the reaction-diffusion model described in the Supp. Mat.

that $\alpha'/\alpha$ is rather equal to 2.12, leading to a prediction plotted as a dashed line ; it predicts correctly the velocity at moderate concentrations, but overestimates the velocity at large concentrations. Redoing for each concentration the calculation of Thomas et al. [24], but considering now the presence of all species and reactions including $HCO_3^-$ (see the detail of the calculations in the Supp. Mat., which includes Refs. [35, 36]), leads to the prediction plotted as a solid line in Fig. 5, which fits the experimental data extremely well except for the last two points. That tiny discrepancy at very large concentrations could be due to saturation of the flux of $CO_2$ above the free surface or to kinetic limitations to the reactions.

Finally, the plume's width is also plotted in Fig. 5(b) as a function of the concentration of NaOH. There is a fair agreement between the experiments and the model

$$\frac{l^{\rm th}}{l_0^{\rm th}} = \Gamma^{-1}\left(1+\frac{\alpha' C_{\rm NaOH}}{\alpha k_{\rm H} P_{\rm CO_2}}\right)^{-1/6} \tag{8}$$

despite large uncertainties in the experimental data. Note that the local Péclet number in the presence of sodium hydroxide $Pe = w_{\max} l/D$ is theoretically equal to $1.156\sqrt{Ra}$.

In conclusion, considering the convective dissolution of $CO_2$ into an aqueous solution of sodium hydroxide (NaOH) in an axisymmetrical geometry and in the late time nonlinear regime, we have measured experimentally the plume's vertical velocity and shown that it is well matched by a theoretical radial profile parametrized by its maximal velocity and width. We have characterized the dependence of the maximal velocity and width of the convective plume on the concentration in NaOH and $CO_2$ pressure, and demonstrated that these dependencies can be explained by a theoretical/analytical model without any adjustable parameter. This was made possible by taking into consideration all the chemical species, their reactions and equilibrium. Consequently, the experimental configuration appears to be a good candidate for a systematic exploration of the convective dissolution of any gaseous species in reactive solution, with the objective, for instance, of maximizing the rate of the potential gaseous absorption (in particular that of $CO_2$) in the quasi-stationary regime.

Prospects to this study include the investigation of porous geometries, where the cylindrical cell will be filled with a transparent granular porous medium whose refractive index is matched by that of the resident solution, as well as different, non-axisymmetrical, confining geometries. In a porous medium, pore scale coupling between heterogeneous advection and molecular diffusion of solute species, which in a passive scalar advection context would result in hydrodynamic dispersion, is also expected to impact the dynamics of the convection [20].

*Acknowledgements:* We thank Anne De Wit for insights, and the Agence Nationale de la Recherche (ANR) for funding of the ANR grant CO2-3D (ANR-16-CE06-0001-01).

* patrice.meunier@univ-amu.fr

[1] A. De Wit, Annu. Rev. Fluid Mech. **52**, 531 (2020).
[2] L. Rongy, P. Trevelyan, and A. De Wit, Phys. Rev. Lett. **101**, 084503 (2008).
[3] Y. Nagatsu, K. Matsuda, Y. Kato, and Y. Tada, J. Fluid Mech. **571**, 475 (2007).
[4] T. Radko, *Double-diffusive convection* (Cambridge University Press, 2013).
[5] P. M. J. Trevelyan, C. Almarcha, and A. De Wit, Phys. Rev. E **91**, 023001 (2015).
[6] X.-Z. Kong and M. O. Saar, Int. J. Greenh. Gas Con. **19**, 160 (2013).
[7] I. Cherezov and S. S. Cardoso, Phys. Chem. Chem. Phys. **18**, 23727 (2016).
[8] V. Loodts, B. Knaepen, L. Rongy, and A. De Wit, Phys. Chem. Chem. Phys. **19**, 18565 (2017).
[9] C. Almarcha, P. M. Trevelyan, P. Grosfils, and A. De Wit, Phys. Res. Lett. **104**, 044501 (2010).
[10] W. E. Ranz, AIChE Journal **25**, 41 (1979).
[11] P. Meunier and E. Villermaux, J. Fluid Mech. **662**, 134 (2010).
[12] A. Bandopadhyay, T. Le Borgne, Y. Méheust, and M. Dentz, Adv. Water Resour. **100**, 78 (2017).
[13] J. A. Neufeld, M. A. Hesse, A. Riaz, M. A. Hallworth, H. A. Tchelepi, and H. E. Huppert, Geophys. Res. Lett. **37** (2010).
[14] H. Huppert and J. Neufeld, Annu. Rev. Fluid Mech. **46**, 255 (2014).
[15] J. Fernandez, P. Kurowski, P. Petitjeans, and E. Meiburg, J. Fluid Mech. **451**, 239 (2002).
[16] S. Backhaus, K. Turitsyn, and R. Ecke, Phys. Review Lett. **106**, 104501 (2011).
[17] C. W. MacMinn, J. A. Neufeld, M. A. Hesse, and H. E. Huppert, Water Resour. Res. **48** (2012).
[18] H. Emami-Meybodi, H. Hassanzadeha, C. Green, and J. Ennis-King, Int. J. Greenh. Gas Con. **40**, 238 (2015).
[19] S. Mahmoodpour, B. Rostami, M. R. Soltanian, and M. A. Amooie, Phys. Rev. Appl. **12**, 034016 (2019).
[20] C. Brouzet, Y. Méheust, and P. Meunier, Phys. Rev. Fluids **7**, 033802 (2022).
[21] J. Dhar, P. Meunier, N. F., and Y. Méheust, Phys. Fluids , 064114 (2022).
[22] V. Loodts, C. Thomas, L. Rongy, and A. De Wit, Phys. Rev. Lett. **113**, 114501 (2014).
[23] M. Budroni, C. Thomas, and A. De Wit, Phys. Chem. Chem. Phys. **19**, 7936 (2017).
[24] C. Thomas, V. Loodts, L. Rongy, and A. De Wit, Int. J. Greenh. Gas Con. **53**, 230 (2016).
[25] D. Avnir and M. Kagan, Nature **307**, 717 (1984).
[26] O. Citri, M. L. Kagan, R. Kosloff, and D. Avnir, Langmuir **6**, 559 (1990).
[27] P. M. Trevelyan, C. Almarcha, and A. De Wit, J. Fluid Mech. **670**, 38 (2011).
[28] F. Nadal, P. Meunier, B. Pouligny, and E. Laurichesse, J. Fluid Mech. **719**, 203 (2013).
[29] P. Meunier and T. Leweke, Exp. Fluids **35**, 408 (2003).
[30] P. Meunier and F. Nadal, J. Fluid Mech. **855**, 1 (2018).
[31] D. M. Himmelblau and A. Babb, AIChE J. **4**, 143 (1958).
[32] H. Hikita, S. Asai, and T. Takatsuka, Chem. Eng. J. **11**, 131 (1976).
[33] H. Hikita, S. Asai, and T. Takatsuka, Chem. Eng. J. **4**, 31 (1972).
[34] A. Hebach, A. Oberhof, and N. Dahmen, J. Chem. Eng. Data **49**, 950 (2004).
[35] R. V. Bhat, J. Kuipers, and G. Versteeg, Mass transfer with complex chemical reactions in gas–liquid systems: two-step reversible reactions with unit stoichiometric and kinetic orders, Chem. Eng. J. **76**, 127 (2000).
[36] C. Almarcha, P. M. Trevelyan, P. Grosfils, and A. De Wit, Thermal effects on the diffusive layer convection instability of an exothermic acid-base reaction front, Phy. Rev. E **88**, 033009 (2013).